



Transport of NH_4NO_3 Aerosols in a Corona Radical Injection Reactor

Marek KOCIK^{*1}, Mirosław DORS^{*}, Jerzy MIZERACZYK^{*}, Janusz PODLIŃSKI^{*},

Seiji KANAZAWA^{**}, Toshikazu OHKUBO^{**}, Jen-Shih CHANG^{***}

(Received September 11, 2003; Accepted January 9, 2004)

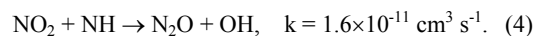
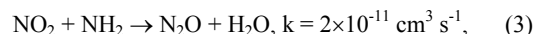
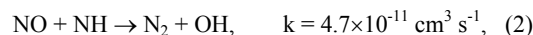
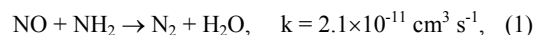
In this paper results of the Particle Image Velocimetry (PIV) investigation of the transport of NH_4NO_3 aerosols produced in a corona radical injection (CRI) reactor during NO_x removal process are presented. The PIV investigation, in which NH_4NO_3 aerosols were employed as tracers, showed that NH_4NO_3 aerosols were transported and distributed in the CRI reactor by the EHD secondary flow (ionic wind). The flow structures generated in the CRI reactor are similar to those found in other corona discharge reactors. The deposition of NH_4NO_3 aerosols in the CRI reactor was not homogeneous. The highest density of the deposited NH_4NO_3 aerosols was on the plate electrode surface where the corona discharge streamers terminated. This was caused by a high velocity of NH_4NO_3 aerosols on their way from the nozzle electrode to the plate electrode.

1. Introduction

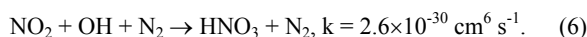
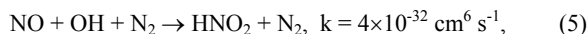
Over the last ten years investigations carried out in laboratories and pilot plants showed that removal of NO_x from flue gases by corona discharges may be very efficient^{1,2}. Many recent investigations have been focused on the performance improvement of the corona discharge processing by optimizing the power source³, using various gaseous additives⁴⁻⁶ or combining the corona discharge processing with other methods⁷⁻⁹.

Among many corona discharge types, the most efficient in NO_x removal is a corona radical shower (CRS) or corona radical injection (CRI)¹⁰⁻¹⁴. In the CRI reactor, a radical precursor gas is introduced into the main flow of the NO_x polluted gas. The radicals produced by the corona enhance NO_x removal. Mostly ammonia is employed as a radical precursor. NH_3 is introduced through a hollow needle electrode into the corona discharge zone where NH_3 molecules dissociate to NH_2

and NH radicals. These radicals assist both reduction and oxidation of NO_x molecules. NO_x molecules are reduced as follows^{13,15}:



OH radicals produced in reactions (2) and (4) oxidize NO and NO_2 into nitric acids in the following reactions:



Once HNO_x molecules are formed, ion induced aerosol particle formation will be initiated^{13,15} in the form of heterogeneous nucleation, together with aerosol particle surface reactions with adsorbed ammonia to form solid ammonium nitrate NH_4NO_3 :



The record NO_x removal energy yield of the CRI method is 40-250 g/kWh at NO_x removal of 95-100 %.

This work was aimed at studying the production and movement of NH_4NO_3 aerosols produced in a corona radical shower reactor. The study was carried out using the Particle Image Velocimetry (PIV) technique. NH_4NO_3 aerosols were expected to be tracers sufficiently good for the PIV measurements. In addition to the fundamental interest in the NH_4NO_3 aerosol behaviour in the corona radical shower reactors, this investigation is related to the topical question - where NH_4NO_3 aerosols are produced, in the discharge region or outside it.

Key words: corona radical injection, secondary flow, PIV, streamer, NH_3NO_4 aerosol

* Centre for Plasma and Laser Engineering, Institute of Fluid Flow Machinery, Polish Academy of Sciences, Fiszerza 14, 80-231 Gdańsk, Poland

** Department of Electrical and Electronic Engineering, Oita University, 700 Dannoharu, Oita 870-1192, Japan

*** Department of Engineering Physics, McMaster University Hamilton, Ontario, L8S 4M1 Canada

¹kocik@imp.gda.pl

2. Experimental set-up

A schematic of the experimental apparatus is shown in Fig. 1. The CRI reactor was an acrylic rectangular reactor (100 mm x 125 mm x 700 mm). A brass hollow needle (2 mm outer diameter, 1.6 mm inner diameter) was used as a CRI electrode. The grounded electrode was a stainless-steel plate. The distance between the electrodes was either 30 mm or 50 mm. DC high voltage with positive polarity was applied through a 10 M Ω resistor to the CRI electrode.

Two gas flows, the main and the additional, were established in the reactor similarly like in the experiment of the CRS^{14, 16}. The main gas (dry air with NO) flowed along the reactor with a flow rate of 3 L/min. The additional gas [dry air with NH_3 and Ar (1.0 %)] was injected through the hollow needle into the main gas flow with a flow rate of 0.5 L/min. The concentration of NO as well as NH_3 in the experiment of Kanazawa *et al.*¹⁶ was 200 ppm. However, at these concentrations of NO and NH_3 the density of NH_4NO_3 aerosols produced in our experiment was too low to employ them as tracers in the PIV measurements. Thus, we increased NO and NH_3 concentrations to 0.5 %.

FTIR analysis of a liquid sample made by solving white powder produced in the reactor proved that no other aerosols than NH_4NO_3 existed in the system. Also the ion-

chromatography analysis of the sample shows the NH_4^+ and NO_3^- ions¹⁴. The size of the aerosols, as laser light reflection measurement showed, was below 1 μm .

The PIV equipment consisted of a twin second harmonic Nd-YAG laser system ($\lambda=532$ nm, pulse energy 50 mJ), imaging optics (a cylindrical telescope), CCD camera, image processor (Dantec PIV 1100), and PC computer. The laser sheet of a thickness of 1 mm, formed from the Nd-YAG laser beam by a cylindrical telescope was introduced into the CRI reactor, perpendicularly to the plate electrode. The NH_4NO_3 particle images were recorded by the Kodak Mega Plus ES 1.0 CCD camera, which captured two images with a time separation of 600 μs . The CCD camera active element size was 1008x1018 pixels. The captured images were transmitted by the Dantec PIV 1100 image processor to the PC computer for digital analysis. The final result of this analysis were maps of the velocity field of NH_4NO_3 aerosols.

When the interelectrode distance was 30 mm, the velocity field maps presented in this paper are composed of several adjacent velocity fields (2 or 4 fields), each of an area of 25 x 25 mm. At the interelectrode distance of 50 mm, each velocity field map is a single field of an area 50 x 50 mm. All the presented velocity field maps resulted from the averaging of 15-25 measurements, i.e. the velocity maps are time-averaged. Measurement error of calculating velocity values is up to 4 %.

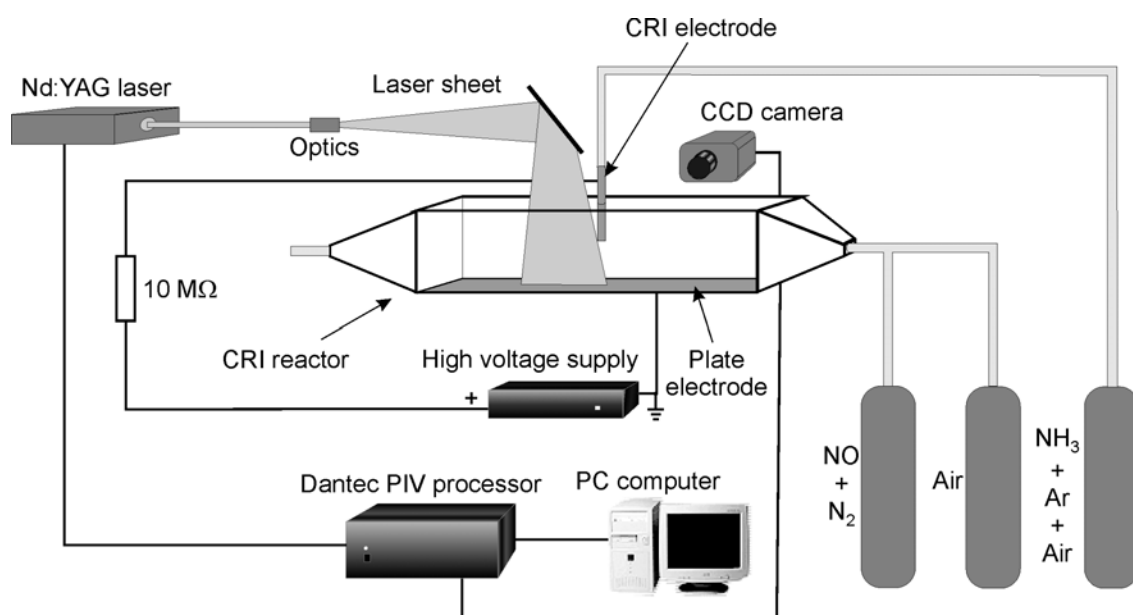


Fig. 1. Experimental set-up.

3. Results

The corona discharge generated in the CRI reactor was not uniformly distributed around the hollow needle edge. The corona discharge is shown in Fig. 2 as a narrow conical streamer starting from one point at the hollow-needle edge the position of which changed irregularly.

The main consequence of such nature of the corona discharge is that velocity field patterns of NH_4NO_3 aerosols measured by PIV are not symmetric in relation to the hollow needle. The asymmetry increases with increasing distance between the hollow needle and plate electrode.

We observed that without the high voltage applied to the hollow needle electrode, NH_4NO_3 aerosols were not produced in the reactor. Their production started when the glow corona discharge mode was established. However, the efficient production of NH_4NO_3 aerosols started in the streamer corona discharge mode, when an optimum voltage was set as in¹⁶⁾. This

optimum voltage was 24 kV and 33 kV at an interelectrode distance of 30 mm and 50 mm, respectively. In both cases the corona discharge current was about 300 μA . All the PIV measurements were carried out at the optimum voltage.

When interelectrode distance was 30 mm, the bulk NH_4NO_3 aerosols move in the entire measurement area more or less perpendicularly to the plane electrode with the highest velocities in the discharge region just below the hollow needle (up to 4 m/s, Fig. 3). Reynolds (Re) and electrohydrodynamical (N_{EHD}) numbers estimated for the region just at the hollow needle outlet are 550 and 7×10^6 , respectively. Since the ratio N_{EHD}/Re^2 is much higher than 1, transport of NH_4NO_3 aerosols is controlled by the EHD-induced secondary flow. As the flow field pattern shown in Fig. 3 resulted from averaging of 20 individual measurements, lasting 6 s in total, the position of the streamer on the nozzle could randomly vary.

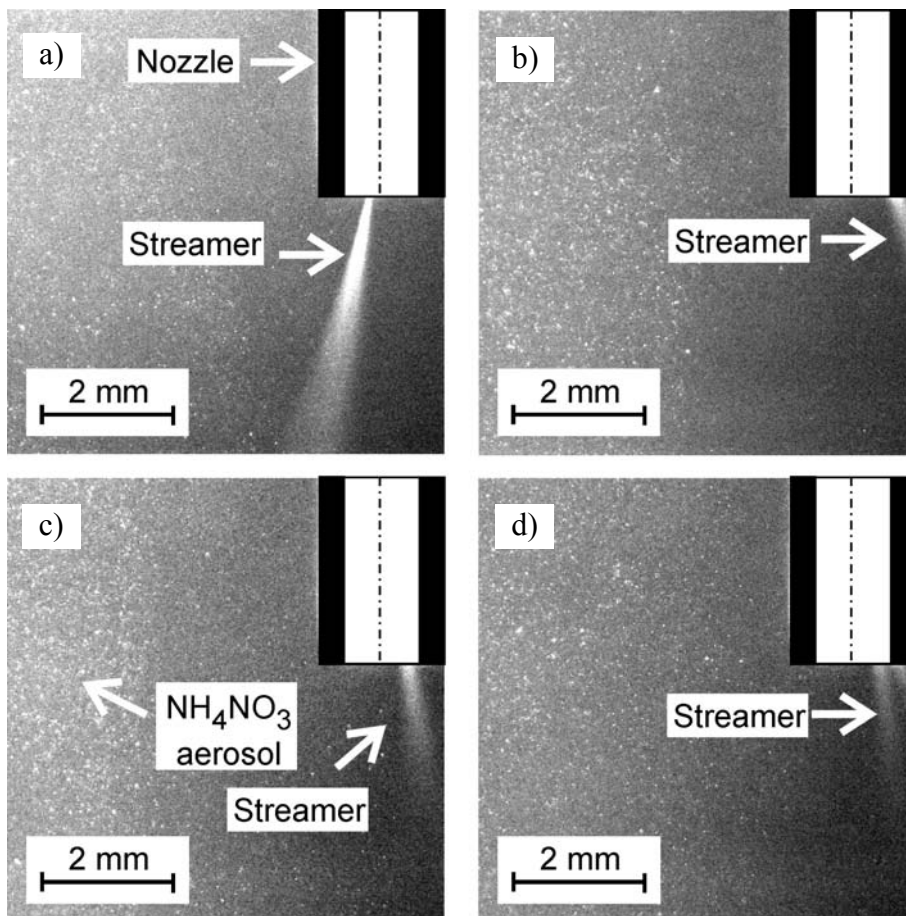


Fig. 2. Typical (we chosen them from a number of photos so that to show different points on the hollow needle edge from which corona streamer developed) temporal images of the downstream area around the hollow-needle during corona discharge. Exposure

time of each image was 133 ns. Interelectrode distance 30 mm. The main flow comes from the right side. NH_4NO_3 solid dust is shown.

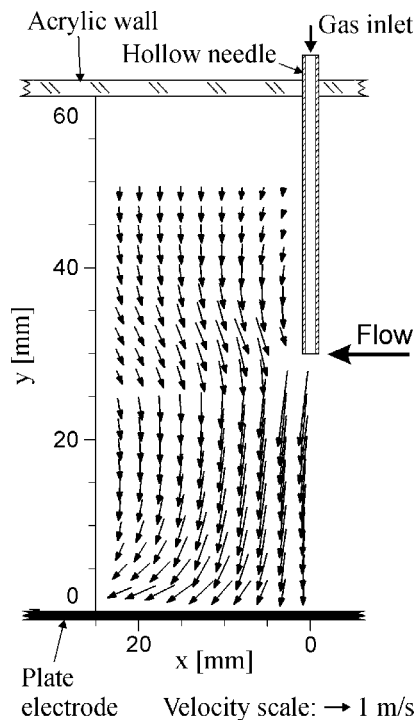


Fig. 3. Flow velocity field downstream of the hollow needle in the CRI reactor. Main gas [air:NO(0.5%)] flow rate - 3 l/min, additional gas [air:Ar(1.0%): NH_3 (0.5 %)] flow rate - 0.5 l/min. The distance from the hollow-needle to the plate electrode - 30 mm. Applied voltage and corona discharge current - 24 kV and 300 μA , respectively (x – horizontal distance from the position of the hollow-needle electrode).

As it is shown in Fig. 3, NH_4NO_3 aerosols flow first along the corona discharge and then along the plate electrode outwards. The relatively fast flow along the corona discharge disturbs electrohydrodynamically the main flow¹⁷⁾ in the reactor ($\text{Re}=8$, $N_{\text{EHD}}=5.9 \times 10^6$), causing formation of large vortices, both downstream and upstream of the hollow needle, as seen in Figs. 4a and 4b. The vortices are formed about 75 mm from the hollow needle. The similar vortices were found in a needle-to-plate corona discharge reactor through which dry air (without NO and NH_3) flowed¹⁷⁾.

The bulk NH_4NO_3 aerosols circulates in the whole measurement area towards the corona discharge region, following the electrohydrodynamically disturbed flow pattern. It gives impression of sucking NH_4NO_3 aerosols present in the reactor by the fast flow directed towards the corona discharge region. After the experiment, it was found that NH_4NO_3

aerosols deposited the whole inner surface of the CRI reactor and also outer reactor ducts.

At the distance between the hollow needle and plate electrode of 50 mm the asymmetry of velocity field patterns of NH_4NO_3 aerosols in relation to the hollow-needle is well pronounced (Fig. 5). The highest velocities of NH_4NO_3 aerosols downstream of the hollow needle electrode are twice than those upstream (4 m/s against 2 m/s, respectively).

4. Conclusions

In this paper results of the PIV measurements of the transport of NH_4NO_3 aerosols produced in the CRI reactor during NO_x removal process are presented for the first time.

The results showed that:

- NH_4NO_3 aerosols can be employed as tracers for PIV measurements;
- NH_4NO_3 aerosols are transported and distributed in the CRI reactor by the EHD secondary flow (ionic wind);
- Flow structures generated in the CRI reactor are similar to those found in other corona discharge reactors;
- Deposition of NH_4NO_3 aerosols in the CRI reactor was not homogeneous. The highest density of deposited NH_4NO_3 aerosols was on the plate electrode surface below the nozzle electrode. This was caused by a high velocity of NH_4NO_3 aerosols in the corona discharge region, directed more or less perpendicularly to the plate electrode.

From the obtained results it is difficult to answer where NH_4NO_3 aerosols were produced: in the corona discharge region or outside it. NH_4NO_3 aerosols were present in the entire measurement area, also very close to the hollow needle outlet. This means that they might be either produced in the corona discharge region or transported to the vicinity of the nozzle by the electrohydrodynamically generated vortices. Thus, the question on the place of NH_4NO_3 aerosols origin is still open. It must be noticed that the PIV measurements of the velocity field were carried out only in one plane, passing through the hollow needle, parallel to the reactor side walls. To know the comprehensive flow velocity field pattern in the reactor, three dimensional map of the velocity field has to be measured.

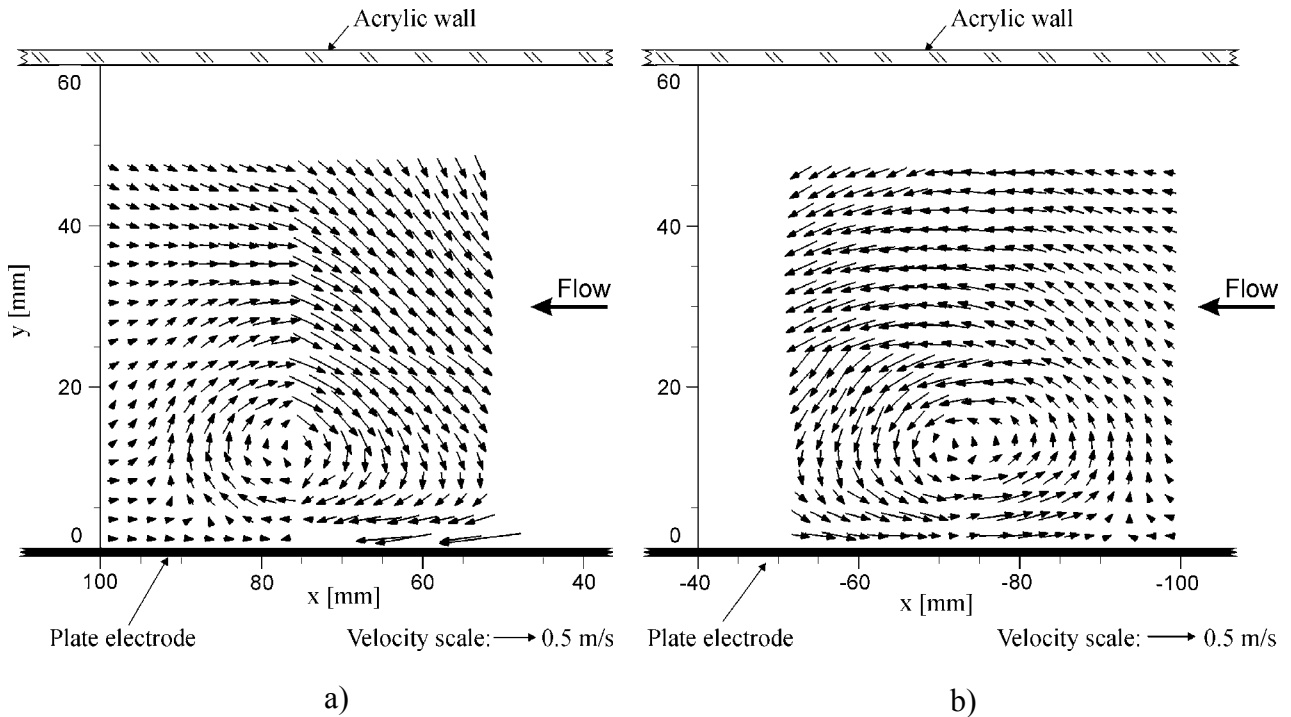


Fig. 4. Flow velocity fields in a distance of 50-100 mm from the hollow needle in the CRI reactor: a) downstream, and b) upstream. Main gas [air:NO(0.5%)] flow rate - 3 l/min, additional gas [air:Ar(1.0%):NH₃(0.5 %)] flow rate - 0.5 l/min. The distance from the hollow-needle to plate electrode - 30 mm. Applied voltage and corona discharge current - 24 kV and 300 μ A, respectively. x - horizontal distance from the position of the hollow-needle electrode.

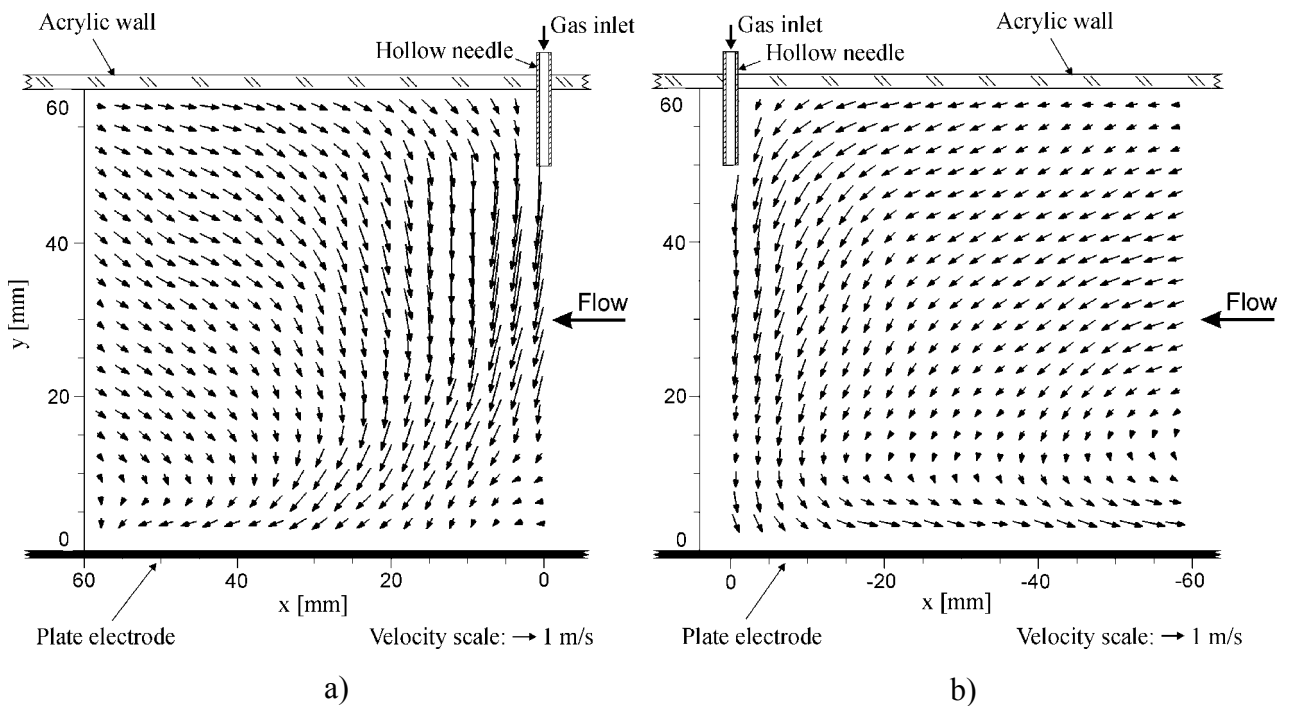


Fig. 5. Flow velocity field in the CRI reactor: a) downstream, and b) upstream. Main gas [air:NO(0.5%)] flow rate - 3 l/min, additional gas [air:Ar(1.0%):NH₃(0.5 %)] flow rate - 0.5 l/min. The distance from the hollow-needle to the plate electrode - 50 mm. Applied voltage and corona discharge current - 33 kV and 300 μ A, respectively. x - horizontal distance from the position of the hollow-needle electrode.

References

- 1) J.S. Chang, in: Non-thermal Plasma Techniques for Pollution Control, Eds. B.M. Penetrante and S.E. Schultheis, Springer-Verlag Berlin Heidelberg, NATO ASI Series, **vol. G 34 (A)**, (1993), pp. 1-32
- 2) E. M. Van Veldhuizen, *Electrical Discharges for Environmental Purposes*, Nova Science Publishers, New York, (2000)
- 3) K. Yan, E. van Heesch, A. Pemen, P. Huijbrechts, F. van Gompel, H. van Leuken, Z. Matyas, *IEEE Trans. Ind. Appl.*, **38**, (2002), pp. 866-872
- 4) A. Mizuno, K. Shimizu, T. Matsuoka, S. Furuta, *IEEE Trans. Ind. Appl.*, **31**, (1995), pp. 463-467
- 5) G. Dinelli, L. Civitano, M. Rea, *IEEE Trans. Ind. Appl.*, **26**, (1990), pp. 535-541
- 6) K. Onda, K. Kato, Y. Kasuga, *JSME International Journal, Series B*, **39**, (1996), pp. 202-210
- 7) H.H. Kim, K. Takashima, S. Katsura, A. Mizuno, *J. Phys. D: Appl. Phys.*, **34**, (2001), pp. 604-613
- 8) T. Hammer, S. Broer, *Plasma Enhanced Selective Catalytic Reduction of NO_x for Diesel Cars*, Society of Automotive Engineers Technical Paper Series, No. 982428, (1998)
- 9) T. Hammer, S. Broer, *Plasma Enhanced Selective Catalytic Reduction of NO_x in Diesel Exhaust: Test Bench Measurements*, Society of Automotive Engineers Technical Paper Series, No. 1999-01-3633, (1999)
- 10) J.S. Chang, P.C. Looy, K. Nagai, T. Yoshioka, S. Aoki, A. Maezawa, *IEEE Trans. Ind. Appl.*, **32**, (1998), pp. 131-136
- 11) J.S. Chang, K. Urashima, M. Arquilla, T. Ito, *Combust. Sci. and Tech.*, **133**, (1998), pp. 31-47
- 12) K. Urashima, J.S. Chang, J.Y. Park, D.C. Lee, A. Chakrabarti, T. Ito, *IEEE Trans. Ind. Appl.*, **34**, (1998), pp. 934-939
- 13) J.Y. Park, I. Tomicic, G.F. Round, J.S. Chang, *J. Phys. D: Appl. Phys.*, **32**, (1999), pp. 1006-1011
- 14) T. Ohkubo, S. Kanazawa, Y. Nomoto, J.S. Chang, T. Adachi, *IEEE Trans. Ind. Appl.*, **30**, 4, (1994), pp. 856-861
- 15) H. Mätzing, *Adv. Chem. Phys.*, **130**, (1991), pp. 315-386
- 16) S. Kanazawa, J.S. Chang, G.F. Round, G. Sheng, T. Ohkubo, Y. Nomoto, T. Adachi, *Combust. Sci. and Tech.*, **133**, (1998), pp. 93-105
- 17) J. Mizeraczyk, J. Dekowski, J. Podliński, M. Dors, M. Kocik, J. Mikielwicz, T. Ohkubo, S. Kanazawa, *IEEE Trans. Plasma Sci.*, **30**, (2002), pp. 164-165